Accepted Manuscript

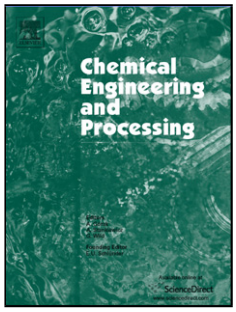

Title: Comparison between phosphine and NHC-modified Pd catalysts in the telomerization of butadiene with methanol – a kinetic study combined with model-based experimental analysis

Author: Lisa Hopf Sebastian Recker Matthias Niedermaier Stephan Kiermaier Vinzent Strobel Dietrich Maschmeyer David Cole-Hamilton Wolfgang Marquardt Peter Wasserscheid Marco Haumann

PII: S0255-2701(15)30060-X
DOI: http://dx.doi.org/doi:10.1016/j.cep.2015.07.007
Reference: CEP 6628

To appear in: *Chemical Engineering and Processing*

Received date: 26-2-2015
Revised date: 12-5-2015
Accepted date: 4-7-2015

Please cite this article as: Lisa Hopf, Sebastian Recker, Matthias Niedermaier, Stephan Kiermaier, Vinzent Strobel, Dietrich Maschmeyer, David Cole-Hamilton, Wolfgang Marquardt, Peter Wasserscheid, Marco Haumann, Comparison between phosphine and NHC-modified Pd catalysts in the telomerization of butadiene with methanol ndash a kinetic study combined with model-based experimental analysis, Chemical Engineering and Processing http://dx.doi.org/10.1016/j.cep.2015.07.007

Comparison between phosphine and NHC-modified Pd catalysts in the telomerization of butadiene with methanol – a kinetic study combined with model-based experimental analysis

Lisa Hopf [1], Sebastian Recker [2], Matthias Niedermaier [1], Stephan Kiermaier [1], Vinzent Strobel [2], Dietrich Maschmeyer [3], David Cole-Hamilton [4], Wolfgang Marquardt [2], Peter Wasserscheid [1], Marco Haumann [1]*,

[1]FAU Erlangen-Nürnberg, Lehrstuhl für Chemische Reaktionstechnik, Egerlandstr. 3, 91058 Erlangen, Germany, Fax: (+49)9131-85-27421, mail: marco.haumann@fau.de

[2]RWTH Aachen University, Aachener Verfahrenstechnik – Process Systems Engineering, Turmstraße 46, 52064 Aachen, Germany

[3]Evonik Industries AG, Paul Baumann Str. 1, 45772 Marl, Germany

[4]EaStCHEM, University of St. Andrews, School of Chemistry, North Haugh, St Andrews, KY16 9ST, United Kingdom

Abstract

The telomerization of butadiene with methanol was investigated in the presence of different palladium catalysts modified either with triphenylphosphine (TPP) or 1,3-dimesityl-imidazol-2-ylidene (IMes) ligand. When pure butadiene was used as substrate, a moderate selectivity for the Pd-TPP catalyst toward the desired product 1-methoxy-2,7-octadiene (1-Mode) of around 87 % was obtained, while the IMes carbene ligand almost exclusively formed 1-Mode with 97.5 % selectivity. The selectivity remained unchanged when the pure butadiene feed was replaced by synthetic crack-C_4 (sCC_4), a technical feed of 45 mol % butadiene and 55 mol % inerts (butenes and butanes). The TPP-modified catalyst showed a lower reaction rate, which was attributed to the expected dilution effect caused by the inerts. Surprisingly, the IMes-modified catalyst showed a higher rate with sCC_4 compared to the pure feed. By means of a model-based experimental analysis, kinetic rate equations could be derived. The kinetic modeling supports the assumption that the two catalyst systems follow different kinetic rate equations. For the Pd-TPP catalyst, the reaction kinetics were related to the Jolly mechanism. In contrast, the Jolly mechanism had to be adapted for the Pd-IMes catalyst as the impact of the base seems to differ strongly from that for the Pd-TPP catalyst. The Pd-IMes system was found to be zero order in butadiene at moderate to high butadiene concentrations and first order in base while the nucleophilicity of the base is influenced by the methanol amount resulting in a negative reaction order for methanol.

Keywords

Telomerization, NHC ligand, TPP ligand, Palladium, reaction kinetics, model-based kinetic analysis

1 Introduction

The telomerization of 1,3-dienes is an important reaction for the synthesis of a variety of bulk and fine chemicals and pharmaceuticals [1]. In its general form, it can be considered as a dimerization of dienes with simultaneous addition of a nucleophile [2, 3]. Industrial applications using 1,3-butadiene as feedstock have been reported by Kuraray Co. Ltd. using water [4] and Dow Chemical using methanol as nucleophile, respectively [5]. The Dow process utilizes a TPP-modified Pd complex and yields 1-methoxy-2,7-octadiene (1-Mode), **1**, as main product with small amounts of 3-methoxy-2,7-octadiene (3-Mode), **2**, and traces of 1,3,7-octatriene, **3**, and vinylcyclohexene, **4**, being formed (see Scheme 1). The 1-Mode is consecutively hydrogenated and the resulting methyloctylether, **5**, is split at elevated temperature into 1-octene, **6**, and methanol, which is recycled back into the process. In the Kuraray process a TPPMS-modified palladium catalyst is used that produces mainly octadien-1-ol, which is then hydrogenated into 1-octanol, an important plasticizer alcohol.

The product composition of both processes can be explained by the mechanism postulated by P.W. Jolly [6] in 1985, depicted in Scheme 2. The catalyst precursor, usually a Pd^{II} salt, is reduced into a Pd^0 complex, **A,** which consecutively exchanges its ligands, L, with 1,3-butadiene to form the active species, **B**. The η^2 bonded butadienes combine to form the C8 alkyl complex, **C,** which, in the presence of methanol, forms transition state **D**. The acidic proton of MeOH is transferred to carbon 6 in the C8 chain to yield complex **E**. In this complex the methoxy group is transferred to either carbon 1 or 3. This transfer determines the selectivity toward products **1** and **2**. Replacement of the η^2,η^2 bonded C8 chain in complex **F** or **F'** by two molecules of 1,3-butadiene yields the product and regenerates the active species, **B**. The side product 1,3,7-octatriene **3** is formed from complex **C** via double bond migration to the terminal position, followed by β-hydride elimination. Vinylcyclohexene **4** is the product of a Diels-Alder reaction of two molecules 1,3-butadiene.

Scheme 1: Telomerization of 1,3-butadiene with methanol according to the Dow Chemical process and consecutive reactions of the major product 1-methoxy-2,7-octadiene [5].

Scheme 2: Proposed reaction mechanism of telomerization, describing the formation of major product **1** and by-products **2** and **3** [6] and introduction of rate constants k_i which are required for kinetic modeling.

In recent years, N-heterocyclic carbene (NHC) ligands have been used to modify the palladium catalyst [7-9]. Compared to the traditional phosphine-modified systems, higher chemo- and regioselectivity and significantly higher activity have been reported.
To the best of our knowledge, all previously reported telomerization catalysts have been applied to either pure 1,3-butadiene feedstock or a technical diluted feed [1, 10-16]. Here we present for the first time a comparative study of both phosphine and NHC-modified palladium catalysts with pure and mixed butadiene feed.

2 Experimental

2.1 Telomerization experiments

All experiments were carried out under inert atmosphere. The catalyst and ligand precursors were stored under inert atmosphere in a Plexiglas® Glovebox (GS GLOVEBOX Systemtechnik GmbH, Argon 4.6). At the start of the reaction, a defined mass of catalyst and ligand were transferred to a Schlenk flask in the Glovebox and afterwards dissolved in a defined mass of methanol. The methanol solutions of catalyst and ligand, base, dibutylether (internal GC standard) and all other used solvents were handled and stored using Schlenk techniques. If not mentioned otherwise, potassium methoxide (KOMe) was used as base.
The batch experiments were carried out in a 250 ml Hastelloy autoclave. The latter was equipped with a four-blade gas entrainment stirrer, a pressure gauge, a pressure relief valve and a heating jacket. The temperature in the vessel was measured with a thermocouple and controlled by a temperature regulator (Horst GmbH, HT MC1) connected to the heating jacket. The autoclave was connected to an argon cylinder as well as to a vacuum pump to ensure inert conditions. All experiments were carried out in the liquid phase. Check valves were implemented to avoid back flow of the reaction mixture into the argon gas cylinder. For starting an experiment, methanol, base, catalyst and ligand solutions and all other required solvents were filled in syringes and introduced to the reaction vessel via a blind plug on top of the autoclave. This mixture was heated up to reaction temperature under stirring. As soon as the reaction temperature was reached, butadiene was added to the autoclave. For this, liquefied butadiene was weighed into a ballast vessel by means of an HPLC pump with cooled pump head. The ballast vessel was connected to the periphery of the autoclave and pressurized to the desired reaction pressure using inert argon gas. As soon as the liquefied butadiene entered the autoclave by opening the respective valves, the reaction started. Samples were taken every 30 minutes via a sampling valve at

the bottom of the reaction vessel. After the final reaction time the stirring was stopped, the autoclave was depressurized, opened and emptied. After cleaning the autoclave, the latter was reassembled and evacuated for at least 1 hour in preparation of the next experiment.

All samples were analyzed with a Varian 3900 gas chromatograph (GC) equipped with either a wall-coated open tubular fused silica column (FS-OV-1-PONA, 50 m x 0.2 mm; C-S Chromatographie Service GmbH) or a column manufactured by Agilent Technologies (CP-Sil PONA CB 50 m x 0.21 mm x 0.5 µm). The injector temperature was set to 250 °C. Helium was used as carrier gas with a flow rate of 1 $ml \cdot min^{-1}$. The products were analyzed by a flame ionization detector (FID) with a temperature of 300 °C. Qualitative analyses were performed using a Varian 450 GC equipped with a Varian VF-5ms column (30 m x 0.25 m) and a Varian 220 MS (ion trap mass spectrometer) with electron ionization.

Figure 1: Schematic flowsheet of the batch autoclave setup manufactured at FAU in Erlangen.

2.2 Model-based experimental analysis

Model-based kinetic investigations of catalytic reactions constitute an essential part of fundamental mechanistic studies [17, 18]. Such studies not only provide insight regarding the evolution of the concentration of the reactants, but also allow for a better understanding of the reaction mechanism and for the determination of reaction rate and equilibrium constants. However, the analysis of experimental data in multistep catalytic reactions is often complicated due to the complexity of the reaction rate law; therefore, simplified reaction kinetic models are often desired to represent concentration data. For such complex reaction systems, dynamic parameter estimation problems are often formulated to estimate the unknown parameters in the rate models [19]. The structure of the reaction kinetic model embedded in this parameter estimation problem is postulated using a priori knowledge on possible reaction mechanisms. The model is fitted to experimental data by adjusting the unknown model parameters such that the deviation between the concentrations predicted by the model and the measured concentration data is minimized. This so-called simultaneous model identification is capable to handle reaction systems of arbitrary complexity. However, if an incorrect model structure is assumed (i.e. if some of the kinetic laws are structurally wrong), an erroneous overall model prediction is obtained and the model error might be difficult to attribute to a particular model-part. To overcome these well-known problems, Marquardt and co-workers suggested an alternative methodology, the so-called incremental model identification (IMI for short), which decomposes the model identification problem in a sequence of properly chosen steps (see [20] or [21] for a tutorial overview). In this work, we utilize the particular stepwise problem decomposition strategy proposed by Brendel *et al.* [22] and adapt it to allow an analysis of the underlying catalytic reaction mechanism:

In a first step, the time-variant reaction fluxes for the various species are estimated from the noisy experimental concentration data. While the reaction flux is often estimated by simple finite difference approximations from concentration data measured at adjacent sampling points [17], the ill-posedness of this inverse problem and the resulting amplification of the errors present in the concentration data is well-known [23]. Special care has to be taken, in particular, if only a limited number of error-prone data points are available in each of the experiments. In this work, we employ a filter-based approach [23] to estimate the reaction fluxes, which successfully controls the amplification of the measurement errors in the concentration data [24]. The individual reaction rates are then calculated from the estimated reaction fluxes using the generalized inverse of the stoichiometry matrix. Subsequently, the reaction rates and the concentration data are correlated by nonlinear regression using a set of candidate reaction rate model structures. The most suitable model structure is selected in a subsequent step from the list of candidates ranked by means of Akaike weights [25], and graphically evaluated by reaction progress kinetic analysis [17].

In a second step, a parameter estimation problem is set up and solved for the most promising model structure identified in the previous step. This way, statistically sound parameter values and their

corresponding confidence intervals can be obtained. Throughout this analysis, profound insight can be accumulated which can be used to elucidate a possible underlying reaction mechanism.

3 Results and discussion

3.1 Parameter variation

The two literature-known ligands, triphenylphosphine (TPP) **7** and 1,3-dimesityl-imidazol-2-ylidene (IMes), **9**, see Scheme 3, were tested in the Pd-catalyzed telomerization reaction using $Pd(acac)_2$ as catalyst precursor. The IMes ligand **9** was generated in-situ from the IMes salt **8** by reaction with the base $KOCH_3$.

Scheme 3: Ligands used in the telomerization of butadiene with methanol.

The two resulting palladium catalysts were exposed under identical conditions to two different feeds each. The Pd:L ratio was kept at 1:4 for all experiments, as this ratio was identified as optimum common ratio for the four systems (for further details see ESI, Figure S1). KOMe was applied as base. The conversions of pure 1,3-butadiene and synthetic crack-C_4 (sCC_4 for short), a mixture of 45 mol % 1,3-butadiene and 55 mol % butenes and butanes, are shown in Figure 2. The conversion in all experiments was related to the starting amount of 1,3-butadiene. In addition, the converted moles of 1,3-butadiene are depicted as a function of reaction time.

Figure 2: Conversion (left) and moles of converted butadiene (right) for experiments with pure 1,3-butadiene (solid symbols) and diluted sCC_4 (open symbols) catalyzed by TPP (triangles) and IMes (squares) -modified palladium systems (7 Pd-TPP+pure butadiene, 8 Pd-TPP+sCC_4, ! Pd-IMes+pure butadiene, ∀ Pd-IMes+sCC_4). In the right diagram, the dashed line indicates the total amount of available butadiene in pure butadiene feed, the solid line indicates the total amount of available butadiene in sCC_4 feed.
Reaction conditions: 70 °C, 15 bar, $V_{reaction}$ = 140 ml, $n_{butadiene}$:n_{MeOH} = 0.5, $n_{butadiene}$:n_{Pd} = 40000, n_{Liq}:n_{Pd} = 4, $n_{butadiene}$:n_{base} = 400, $c_{Pd,0}$ = 0.15 mmol·l^{-1} and $c_{butadiene,0}$ = 6.1 mol·l^{-1} for experiments with pure butadiene, $c_{Pd,0}$ = 0.086 mmol·l^{-1} and $c_{butadiene,0}$ = 3.4 mol·l^{-1} for experiments with sCC_4.

For pure 1,3-butadiene, the initial reaction rate was higher for the Pd-TPP system compared to the Pd-IMes one. However, after 1.5 h of reaction time, the reaction rate slowed down at about 70 % conversion, probably caused by catalyst deactivation. In addition, at low concentrations of 1,3 butadiene, the equilibrium could be shifted from the active species **B** toward the ligand substituted Pd^0 species **A**. This would lower the concentration of active palladium centers in the system and slow down the reaction rate. With the diluted sCC_4 feed, the reaction started with a lower rate compared to pure butadiene. After 6 h and a conversion of the reactive butadiene fraction of around 70 %, the activity of the system decreased strongly. The lower reaction rate for the Pd-TPP system is probably due to this dilution effect.
In contrast, the Pd-IMes system yielded full conversion after 4.5 h for the pure 1,3-butadiene feed. Compared to the explanation for the TPP ligand, this could stem from the fact that the palladium is not able to coordinate more than one bulky IMes ligand and therefore the equilibrium between species **A** and **B** is in favor of the active species **B**. Even more surprisingly, the conversion of the IMes-modified palladium catalyst increased when diluted sCC_4 feed was used and full conversion was obtained within 4 h. This behavior was reproduced several times and the trend has also been seen using a reactor with a fivefold larger reaction volume.
By plotting the amount of converted 1,3-butadiene versus reaction time, the resulting rate for the Pd-IMes catalyst is independent of the applied feed in the first hours. With the diluted feed, the rate levels off after around 3.5 hours. The amount of converted 1,3-butadiene is lower due to the lower

amount of 1,3-butadiene present in the diluted feed. For the Pd-TPP catalyst the reaction rate with pure butadiene is higher than with sCC_4 confirming the assumed dilution effect.

As summarized in Table 1, the selectivity to the desired product **1** was significantly higher for the IMes-modified catalyst system and seemed to be independent of the applied feed. For TPP, the selectivity to **1** differed slightly for the two feeds and was higher for pure butadiene.

Compared to the TPP ligand, the IMes-modified systems showed a distinctively lower selectivity to the byproducts **2**, **3** and vinylcyclohexene **4**, resulting in a higher *n*:*iso* ratio. The formation of byproducts with Pd-TPP was probably due to the higher sensitivity of the TPP system to an excess of ligand due to its lower steric demand [9]. For the TPP system, the coordination of a second ligand is facilitated leading to lower 1-Mode selectivity as reported by Vollmüller *et al.* [10].

In order to investigate the origin of the higher activity of the diluted feed, pure 1,3-butadiene was combined with a) an inert solvent and b) a component of the sCC_4 to mimic the dilution of butadiene in sCC_4. For these experiments hexane and toluene were applied, which both should be chemically inert in the telomerization of butadiene with methanol. *Iso*-butene, one of the main components of the sCC_4 mixture, was tested as well. The results for both modified catalysts are shown in Figure 3. Additionally, *n*-butane and 1-butene were used as inert compounds for the IMes-modified palladium catalyst showing similar results as those for *iso*-butene (see ESI, Figure S2).

Figure 3: Conversion in Pd-TPP (left) and Pd-IMes (right) catalyzed telomerization of pure 1,3-butadiene (!), sCC_4 (∀) and 1,3-butadiene diluted with hexane (8), toluene (–) and *iso*-butene (X).
Reaction conditions: 70 °C, 15 bar, $V_{reaction}$ *= 140 ml,* $n_{butadiene}:n_{MeOH}$ *= 0.5,* $n_{butadiene}:n_{Pd}$ *= 40000,* $n_{Lig}:n_{Pd}$ *= 4,* $n_{butadiene}:n_{base}$ *= 400,* $c_{Pd,0} = 0.15\ mmol \cdot l^{-1}$ *and* $c_{butadiene,0} = 6.1\ mol \cdot l^{-1}$ *for experiment with pure butadiene,* $c_{Pd,0} = 0.086\ mmol \cdot l^{-1}$ *and* $c_{butadiene,0} = 3.4\ mol \cdot l^{-1}$ *for experiments with* sCC_4*/diluted feeds.*

For the Pd-TPP system, the highest activity was obtained for pure 1,3-butadiene as substrate, all diluted substrates showed reduced activity similar to the one for sCC_4. No difference between an inert solvent or *iso*-butene could be observed. The values for the selectivity to the main product, the chemoselectivity as well as the *n*:*iso* ratios were nearly the same for hexane, toluene and *iso*-butene as additional solvent. The diluted systems showed a minor incubation period of approx. 1 h, after which the reaction proceeded with higher rate. With progressing reaction, the even lower substrate concentration in the batch reactor caused the activity of all diluted systems to level off around 80 % conversion after 6 h.

For the IMes-modified catalyst, the use of pure 1,3-butadiene feed resulted in the lowest reaction rates again, while all other diluting solvents and the sCC_4 gave higher reaction rates. Within the error margin the effect of all diluting solvents on the reaction rate was identical and the rates were the same. The inerts *n*-butane and 1-butene also behaved similar to *iso*-butene (see ESI, Figure S2) and the inert solvents toluene and hexane. This behavior indicates that the Pd-IMes system is either deactivated by too high concentrations of 1,3-butadiene or follows a zero-order reaction kinetics with respect to butadiene.

Interestingly, all other studied Pd-NHC catalysts also showed higher activity for the diluted sCC_4 compared to pure 1,3-butadiene (see ESI, Figures S3 and S4). This indicates that the observed effect is not limited to IMes-modified palladium complexes, but represents a rather general effect for NHC ligands.

The influence of 1,3-butadiene concentration was further studied by varying the molar ratio of methanol to 1,3-butadiene. As no additional inert solvent was used, the molar ratios of all other components were kept constant related to 1,3-butadiene. In consequence, the concentration of several components changed. The goal was to see the influence of the reactant butadiene on the two different catalyst systems at the same conditions. The results for both catalyst complexes with both feeds are depicted in Figure 4.

Figure 4: Influence of the molar ratio of butadiene to methanol for the TPP (left) and the IMes (right) -modified catalysts with pure butadiene (top) and sCC_4 (bottom) (T 2:1, ∀ 1:1, – 1:1.5, 8 1:2, X 1:2.5, Ξ 1:3, ; 1:5).
Reaction conditions: 70 °C, 15 bar, $V_{reaction} = 140$ *ml,* $n_{butadiene}:n_{Pd} = 40000$, $n_{Lig}:n_{Pd} = 4$, $n_{butadiene}:n_{base} = 400$.
Experiments with pure butadiene: T *2:1:* $c_{butadiene,0} = 9.3\ mol \cdot l^{-1}$, ∀ *1:1:* $c_{butadiene,0} = 7.9\ mol \cdot l^{-1}$, – *1:1.5:* $c_{butadiene,0} = 6.6\ mol..l^{-1}$, 8 *1:2:* $c_{butadiene,0} = 5.9\ mol..l^{-1}$, X *1:2.5:* $c_{butadiene,0} = 5.3\ mol \cdot l^{-1}$, Ξ *1:3:* $c_{butadiene,0} = 4.6\ mol \cdot l^{-1}$, ; *1:3:* $c_{butadiene,0} = 3.5\ mol \cdot l^{-1}$.
Experiments with sCC_4*:* T *2:1:* $c_{butadiene,0} = 4.3\ mol \cdot l^{-1}$, ∀ *1:1:* $c_{butadiene,0} = 4.1\ mol \cdot l^{-1}$, – *1:1.5:* $c_{butadiene,0} = 3.9\ mol \cdot l^{-1}$, 8 *1:2:* $c_{butadiene,0} = 3.6\ mol \cdot l^{-1}$, X *1:2.5:* $c_{butadiene,0} = 3.4\ mol \cdot l^{-1}$, Ξ *1:3:* $c_{butadiene,0} = 3.2\ mol \cdot l^{-1}$, ; *1:3:* $c_{butadiene,0} = 1.4\ mol \cdot l^{-1}$.

Within the range of methanol to 1,3-butadiene from 1:1 to 1:3, no large difference in the performance was observed for the phosphine-based catalyst. The application of a large excess of methanol (1:5) resulted in an activation phase of around 1.5 to 2 hours (see Figure 4, top left diagram, ;). This was probably caused by slower catalyst activation due to the highly diluted catalyst. A negative influence was obtained with a stoichiometric ratio of butadiene to methanol of 2:1. Butadiene is known as a catalyst inhibitor due to its chelating properties. At the stoichiometric ratio, the butadiene concentration is probably too high thereby blocking the catalyst in a chelating fashion.
With the diluted butadiene feed, the activity achieved at all ratios was lower compared to pure butadiene for the Pd-TPP catalyst. Interestingly, a clear trend was observed. An increase in the methanol concentration caused an increase in activity. Regarding the molecularity of the reaction, the reaction would follow a second order in butadiene and a first order in methanol. In consequence, the negative influence of a lower reactants' concentration would be weaker for a first order dependency meaning that the reaction rate increases with increasing concentration of methanol.
For the Pd-IMes catalyst in combination with pure butadiene, a strong dependence on the butadiene to methanol ratio was observed. The increase of the 1,3-butadiene concentration reflected by higher butadiene to methanol ratios resulted in a faster reaction. This behavior is in good agreement with results reported for the telomerization of 1,3-pentadiene using the same Pd-IMes catalyst complex at 70 °C [26]. Here, the authors observed no significant change in final conversion with increasing concentration of 1,3-pentadiene, but the initial reaction rates were increased with higher substrate concentration.
The apparent contradiction between the dependency on the butadiene concentration observed here and the zero-order dependency on butadiene found in the earlier experiments (see above) stems from the fact that, at fixed butadiene to catalyst ratios, the amount of catalyst increased with increasing ratio of butadiene to methanol, as did also the amount of base.
With the diluted feed, an optimum ratio of 1:2 was found. Due to the complexity of this multi-parameter system the exact influence of each individual component could not be determined independently in experiments, thus we applied a model-based experimental analysis to further shed light on this complex system.
The obtained selectivities were independent of the applied feed for both ligands. For the TPP-modified catalyst, the regio- as well as the chemoselectivity increased with increasing amount of methanol, which is again in good agreement with the literature [10].
With the Pd-IMes catalyst high selectivities of 97 to 98 % were achieved toward the main product. The selectivities were not affected by the studied variations except at the stoichiometric ratio. Here, the formation of the main product 1-Mode decreased whereas the selectivity toward 3-Mode and octatriene increased.
All results discussed so far strongly hint at the fact that Pd-catalyzed telomerization catalysis follows fundamentally different reaction kinetics for the TPP and the IMes ligands. Therefore, a closer examination of the observed kinetics for both ligand-modified catalysts was carried out by a model-based experimental analysis.

3.2 Modeling results

3.2.1 TPP ligand

The first step of the applied model-based experimental analysis is, as mentioned before, the calculation of the individual reaction rates from experimental data. Although the stoichiometric matrix of the reactions

$$Pd_{pre} + 2B \xrightarrow{R_0} Pd_{act} \quad , \ (1)$$

$$2B + M + Pd_{act} \xrightarrow{R_1} P + Pd_{act} \quad , \ (2)$$

$$2B + Pd_{act} \xrightarrow{R_2} D + Pd_{act} \ (3)$$

(with B for butadiene, M for methanol, P for the main-product 1-Mode, D for the side-product 3-Mode, Pd_{pre} for the catalyst precursor and Pd_{act} for the activated catalyst) is regular [22], the reaction rate R_0 for catalyst activation cannot be deduced from the available measurements due to two reasons not covered by the structural argument ensuring identifiability: (i) the catalyst activation occurs in the first few minutes of the reaction, where only few measured data points are available; (ii) the influence of this reaction on the 1,3-butadiene concentration is quite low due to small catalyst concentrations. The experimental errors are dominating the concentration measurements, such – even with a higher sampling rate – this reaction rate is not accessible from the data in the suggested experimental setting. Consequently, it is assumed in the following, that the catalyst has already been activated at the start of the reaction. Hence, the competition between the first and the other two reactions for *B* during the very first minutes of the reaction is neglected.

Mechanistic cycles reported for similar reactions in literature can serve as a good starting point for deriving kinetic model candidates. For the telomerization reaction considered here, two different catalytic cycles can be found in literature, the Jolly mechanism [6] and the dipalladium-bisally mechanism [27, 28]. Assuming that the order of each reaction step corresponds strictly to the stoichiometry and that the intermediates show quasi-stationary behavior, the model structures

$$R_1 = [Pd_{act}] \frac{K_1^{Dipa}[M][B]^2}{1 + K_2^{Dipa}[M]} \ (4)$$

$$R_2 = [Pd_{act}] \frac{K_3^{Dipa}[B]^2}{1 + K_4^{Dipa}[M]} \ (5)$$

and

$$R_1 = [Pd_{act}] \frac{K_1^{Jolly}[B]^2[M]}{1 + K_2^{Jolly}[B]^2 + K_3^{Jolly}[B]^4} \ (6)$$

$$R_2 = [Pd_{act}] \frac{K_4^{Jolly}[M][B]^2(1 + K_5^{Jolly}[B]^2)}{1 + K_6^{Jolly}[B]^2 + K_7^{Jolly}[B]^4} \ (7)$$

can be derived for the dipalladium-bisally and the Jolly mechanism, respectively, using the procedure reported in [29]. Note that the parameters in these rate equations are complex nonlinear functions of

the reaction rate constants k_i of the elementary reactions postulated in the reaction mechanism (see Scheme 1). Both model structures show a first-order dependency of the reaction rates R_1 and R_2 of the main and the side reactions respectively, on the catalyst concentration, but a more complex dependency on the reactants' concentrations.

A drawback of such mechanistically motivated model structures is that they are often not identifiable. The identifiability of a model refers to the question whether the model parameters of a given model structure can be determined uniquely from the available set of (perfect) experimental data. The mechanistic models are shown not to be identifiable using the procedure reported in [30] and the parameter identifiability test presented in [31]. Since no additional measurements are possible, identifiability can only be restored by model reduction. The identifiable reduced models

$$R_1 = [Pd_{act}] K_1^{Dipa} [M][B]^2 \quad (8)$$

$$R_2 = [Pd_{act}] K_3^{Dipa} [B]^2 \quad (9)$$

and

$$R_1 = [Pd_{act}] \frac{K_1^{Jolly} [B]^2 [M]}{1 + K_2^{Jolly} [B]^2} \quad (10)$$

$$R_2 = [Pd_{act}] K_4^{Jolly} [M][B]^2 \quad (11)$$

were derived for the dipalladium and the Jolly mechanisms, respectively. These model structures will be used in the subsequent IMI. For comparison, we also consider the empirical model

$$R_1 = K_1^{Emp} [B]^{K_2^{Emp}} [M]^{K_3^{Emp}} [Pd_{act}]^{K_4^{Emp}} \quad (12)$$

$$R_2 = K_1^{Emp} [B]^{K_6^{Emp}} [M]^{K_7^{Emp}} [Pd_{act}]^{K_8^{Emp}} \quad (13)$$

where the reaction orders are treated as model parameters. The parameters of this model can also be shown to be non-identifiable.

Table 2 shows the results of the IMI for the TPP ligand. The models for the reduced Jolly and the reduced dipalladium mechanisms result in Akaike weights which are at least an order of magnitude higher than those of the other three models. Hence, one of these models will most likely qualify as the best model in the sense of Akaike's Information Criterion (AIC). This is consistent with the finding that only the mechanistically motivated, reduced models are identifiable. Hence, the lower Akaike weights of empirical and non-reduced models can be explained by the presence of (additional) non-identifiable parameters.

To allow a graphical inspection by reaction progress kinetic analysis [17] of the two favorable models identified by IMI, the rates for the main reactions were normalized to provide new functions, which only depend on one substrate concentration. For the reduced Jolly mechanism, the rate R_1 of the main reaction is normalized by the catalyst and the methanol concentrations to provide a new function depending only on butadiene concentration:

$$\frac{R_1}{[Pd_{act}][M]} = \frac{K_1^{Jolly}[B]^2}{1 + K_2^{Jolly}[B]^2} = f_1([B]). \quad (14)$$

Likewise, the rate R_1 for the reduced dipalladium mechanism is normalized by the catalyst concentration and by the square of the butadiene concentration to provide a new function depending only on the methanol concentration:

$$\frac{R_1}{[Pd_{act}][B]^2} = K_1^{Dipa}[M] = g_1([M]). \quad (15)$$

Figure 5: Normalized measured reaction rates and identified rate equations (line) for TPP ligand; reduced Jolly mechanism (left); reduced dipalladium mechanism (right). Solid symbols refer to experiments with pure 1,3-butadiene, open symbols to experiments with sCC_4.
Reaction conditions: 70 °C, 15 bar, $V_{reaction}$ = 140 ml, $n_{butadiene}$:n_{Pd} = 40000, n_{Lig}:n_{Pd} = 4, $n_{butadiene}$:n_{base} = 400, $n_{butadiene}$:$n_{methanol}$ = (black = 1:2, red = 1:3, green = 1:1, blue = 1:1.5, pink = 1:2.5).

An evaluation of the validity of the model structures for the reduced Jolly and dipalladium mechanisms is possible, if the normalized reaction rates are plotted as a function of butadiene or methanol, respectively. This graphical inspection, termed as reaction progress kinetic analysis [17], is shown in Figure 5. Different experiments show a much better match with the reduced Jolly mechanism on the left than with the reduced dipalladium mechanism on the right. Hence, this graphical analysis confirms the ranking results of the IMI. Still, the normalized reaction rates do not align completely for the reduced Jolly mechanism (Figure 5, left). The deviations can be explained by the neglected catalyst activation reaction and by experimental errors. A simultaneous parameter estimation has been performed for the more promising reduced Jolly mechanism to obtain statistically sound parameter values and to calculate their corresponding confidence intervals. The parameter estimation is constrained by a dynamic model for the batch experiments consisting of the following mass balance equations:

$$\frac{d[Pd_{pre}]}{dt} = -R_0 \quad (16)$$

for the Pd-precursor concentration,

$$\frac{d[Pd_{act}]}{dt} = R_0 \quad (17)$$

for the active catalyst concentration,

$$\frac{d[B]}{dt} = -2R_1 - 2R_2 \quad (18)$$

for the butadiene concentration,

$$\frac{d[M]}{dt} = -R_1 \quad (19)$$

for the methanol concentration,

$$\frac{d[P]}{dt} = R_1 \quad (20)$$

for the 1-Mode concentration,

$$\frac{d[D]}{dt} = R_2 \quad (21)$$

for the dimer concentration and

$$R_0 = K_0 [B]^2 \left[Pd_{pre} \right] \tag{22}$$

as rate equation for catalyst activation and

$$R_1 = [Pd_{act}] \frac{K_1^{Jolly} [B]^2 [M]}{1 + K_2^{Jolly} [B]^2} \tag{10}$$

$$R_2 = [Pd_{act}] K_4^{Jolly} [M] [B]^2 \tag{11}$$

as rate equations for product formation according to the reduced Jolly mechanism.

For the catalyst activation, the equilibrium between species **A** and **B** was neglected as a consideration in the model did not show an improvement of the fit. In addition, the interaction with the ligand in the step of catalyst activation was not taken into account as the ligand was present in excess in the experiments. In general, the catalyst activation proceeds very fast for both catalyst systems (see ESI, Figure S5).

The resulting parameter estimates and their confidence intervals are shown in

Table 3. The uncertainties represented by the confidence intervals are less than 10 % of the nominal parameter values, except in case of parameter K_0. As discussed before, a reliable estimation of this parameter is difficult, since the reaction rate of the catalyst activation cannot be suitably accessed by the available measurements. For the main reaction, the model exhibits second-order in butadiene and first-order in methanol at moderate to low butadiene concentrations. This is in agreement with the slow reaction progress towards the end of the reaction, especially for the experiments with sCC_4, see Figure 6.

Figure 6: Results of simultaneous parameter estimation for the TPP ligand with the model for reduced Jolly mechanism. Solid symbols and lines refer to experiments with pure 1,3-butadiene, open symbols and dashed lines to experiments with sCC_4.
Reaction conditions: 70 °C, 15 bar, $V_{reaction}$ = 140 ml, $n_{butadiene}$:n_{Pd} = 40000, n_{Lig}:n_{Pd} = 4, $n_{butadiene}$:n_{base} = 400, $n_{butadiene}$:$n_{methanol}$ = (black = 1:2, red = 1:3, green = 1:1, blue = 1:1.5, pink = 1:2.5).

At very high butadiene concentrations, the expression $K_2^{Jolly} [B]^2$ is much larger than 1 meaning that the reaction only depends on the methanol concentration in this range of butadiene concentration. This aligns with the approximately linear butadiene consumption (zero-order dependency) in the first hour of the reaction for all experiments. The dependency on the methanol concentration in the first hour of the reaction means that the addition of methanol in the protonation step from species **C** to **D** respectively **E** is rate limiting. This assumption is in accordance with a DFT calculation by Jabri *et al.* [32]. They proposed the protonation of species **C** to species **E** via intermediate species **D** to be the rate determining step when working at high pH, in our case with the base KOMe.

Since the parameters of the rate equations for the Jolly mechanism ($K_1^{Jolly} - K_7^{Jolly}$) consist of the products of the rate constants of the elementary reaction steps ($k_1 - k_8$)

$$K_1^{Jolly} = \frac{k_1 k_2 k_3 k_4}{k_6 k_7 k_8}\ , \tag{23}$$

$$K_2^{Jolly} = \frac{k_2 k_5}{k_6 k_7} + \frac{k_5}{k_7} + \frac{k_2 k_3 k_4}{k_6 k_7 k_8} + \frac{k_3 k_4}{k_6 k_7 k_8} + \frac{k_4}{k_8}, \quad (24)$$

$$K_3^{Jolly} = \frac{k_2 k_4 k_5}{k_6 k_7 k_8}, \quad (25)$$

$$K_4^{Jolly} = \frac{k_1 k_2 k_5}{k_7 k_8}, \quad (26)$$

$$K_5^{Jolly} = \frac{k_4}{k_6 k_7 k_8}, \quad (27)$$

$$K_6^{Jolly} = \frac{k_2 k_5 k_8}{k_6 k_7} + \frac{k_5 k_8}{k_6 k_7} + \frac{k_2 k_3 k_4}{k_6 k_7} + \frac{k_3 k_4}{k_6 k_7} + k_4, \quad (28)$$

$$K_7^{Jolly} = \frac{k_2 k_4 k_5}{k_6 k_7} + \frac{k_4 k_5}{k_8}, \quad (29)$$

the results of the identifiability analysis can also be utilized to elucidate the rate determining step. Here, K_3^{Jolly}, K_5^{Jolly} and K_7^{Jolly} are not identifiable and can be eliminated without influencing the model behavior. If these parameters are not influencing the reaction rate, they seem to be not involved in the rate determining step. This means that the replacement of the η^2,η^2 bonded C8 chain in complex **F** or **F'** by two molecules of 1,3-butadiene and the butadiene coupling in the formation of octatriene with the rate constants k_4 and k_5 are not rate limiting. In consequence, the steps of methanol bonding and protonation as well as the nucleophilic attack described by k_1 and k_3 are rate determining. These results are also in accordance with the DFT study published by Jabri *et al.* [32].

3.2.2 IMes ligand

The systematic identification approach presented above has also been applied to the catalysis with the IMes ligand. Since the amount of side-product is very small in this case, the rate for the side reaction is set to zero for all model candidates and IMI is performed for the rate equation of the main reaction only.

Table 4 shows the results of the IMI for the IMes ligand. Here, the unidentifiable, empirical model yields the highest Akaike weight, while the Akaike weights for all models resulting from mechanistic considerations are at least an order of magnitude lower. In contrast to the TPP catalyzed reaction, the penalization of the (additional) non-identifiable parameters of the empirical model is more than compensated by the better match with the experimental data. This is consistent with graphical findings from reaction progress kinetic analysis [17] shown in Figure 7, which reveals that neither the normalized reaction rates for the reduced Jolly mechanism nor for the reduced dipalladium mechanism fall on top of each other. It consequently can be concluded that the reaction with the IMes-modified catalyst does not follow the kinetic mechanism observed for the TPP ligand. Therefore, a completely different dependency on the concentrations of the involved components has been derived and studied in further experiments.

Figure 7: Normalized measured reaction rates and identified rate equations (line) for IMes ligand; reduced Jolly mechanism (left); reduced dipalladium mechanism (right). Solid symbols refer to experiments with pure 1,3-butadiene, open symbols to experiments with sCC_4. *Reaction conditions: 70 °C, 15 bar, $V_{reaction}$ = 140 ml, $n_{butadiene}$:n_{Pd} = 40000, n_{Lig}:n_{Pd} = 4, $n_{butadiene}$:n_{base} = 400, $n_{butadiene}$:$n_{methanol}$ = (black = 1:2, red = 1:3, green = 1:1, blue = 1:1.5, pink = 1:2.5).*

The presented experiments with the catalyst using an IMes ligand give some hints for model development. The reaction resembles an overall zero-order dependency of the reactants and seems to be strongly dependent on either the catalyst or the base concentration. To further investigate these effects, additional experiments were carried out. The variation of different components, namely butadiene, base and methanol were conducted by varying the amount of the studied component and keeping everything else constant by using hexane as inert solvent. In addition, the base strength was varied. The experimental results are depicted in Figure 8.

Figure 8: Influence of the concentration of base (top, left), the base strength (top, right), the concentration of butadiene (bottom, left) and the concentration of methanol (bottom, right) on the telomerization reaction using the IMes-modified Pd catalyst.

Base variation: Ξ 23.10 mmol·l^{-1}, X 18.55 mmol·l^{-1}, – 14.36 mmol·l^{-1}, 8 9.24 mmol·l^{-1}, 7 4.77 mmol·l^{-1};

Base strength: Ξ KOMe, X NEt_3, – 10xNEt_3, 8 no base,

Butadiene variation: (7 7.85 mol·l^{-1} ($n_{butadiene}$:n_{MeOH} =1:1), 8 5.23 mol·l^{-1} (1:1.5), – 3.91 mol·l^{-1} (1:2), X 3.14 mol·l^{-1} (1:2.5), Ξ 2.61 mol·l^{-1} (1:3);

Methanol variation: (Ξ 4.85 mol·l^{-1} ($n_{butadiene}$:n_{MeOH} =1:1), X 7.23 mol·l^{-1} (1:1.5), – 9.61 mol·l^{-1} (1:2), 8 11.99 mol·l^{-1} (1:2.5), 7 14.46 mol·l^{-1} (1:3).

Reaction conditions:
Base variation: 70 °C, 15 bar, $V_{reaction}$ = 140 ml, $n_{butadiene}$:n_{MeOH} = 0.5, $n_{butadiene}$:n_{Pd} = 40000, n_{IMes}:n_{Pd} = 4
Base strength: 70 °C, 15 bar, $V_{reaction}$ = 140 ml, $n_{butadiene}$:n_{MeOH} = 0.5, $n_{butadiene}$:n_{Pd} = 40000, n_{IMes}:n_{Pd} = 4, $n_{butadiene}$:n_{base} = 400, $c_{butadiene,0}$ = 6.1 mol·l^{-1}
Butadiene variation: 70 °C, 15 bar, $V_{reaction}$ = 140 ml, n_{MeOH} = 1.1 mol, n_{Pd} = 0.028 mmol, n_{IMes} = 0.111 mmol, n_{KOMe} = 2.58 mmol, solvent: hexane
Methanol variation: 70 °C, 15 bar, $V_{reaction}$ = 140 ml, $n_{butadiene}$ = 0.68 mol, n_{Pd} = 0.017 mmol, n_{IMes} = 0.068 mmol, n_{KOMe} = 1.6 mmol, solvent: hexane.

By variation of the base concentration, a strong influence on the reaction rate was observed resembling a first-order dependency in the base concentration. This strong influence was already discussed in the literature [13]. Furthermore, the variation of the base strength showed that the Pd-IMes catalyst seems to be only efficiently activated by a strong base such as KOMe. The use of no base, NEt_3 as well as the 10-fold amount of NEt_3 exhibited no to only very low (2.5%) conversion values. An increase of the reaction time from 6 to 18 hours resulted in a conversion value of 6 %. This observation is in contradiction to the behavior of the Pd-TPP catalyst (for further details see ESI, Figure S6). Here, the highest activity was obtained with KOMe, but the use of NEt_3 resulted in only slightly lower conversion values. The experiment without base showed a slight activation phase but afterwards reached comparable high activities to the experiments with KOMe and NEt_3.

A change of the butadiene concentration did not show an effect on the reaction rate meaning that the telomerization reaction with the IMes-modified catalyst is of zeroth order in the butadiene concentration.

For the methanol variation, the observed behavior was completely different. The reaction rate decreased with increasing methanol meaning that methanol shows a negative effect on the telomerization reaction. One possible reason for this might be that the nucleophilicity of the base changes with changing methanol concentration. The methoxide anion of the base will possibly be a much better nucleophile at lower concentration of the protic solvent methanol. An alternative is that there is an equilibrium between bound methoxide and bound methanol, either through displacement of bound methoxide by methanol or by protonation of bound methoxide by methanol (these are

kinetically indistinguishable). If only the methoxide complex can carry the mechanistic cycle, this would also give a first-order dependency on base and a dependency on methanol of order -1.
In order to distinguish between these possibilities three experiments were carried out, where the ratio of base to methanol was kept constant. Compared to the previous experiments with varying base to methanol ratio, the reaction rates were increased but were not the same. Again, the experiment with the largest amount of methanol showed the lowest reaction rate. This means that the negative effect of methanol is stronger than the positive effect of the base. This might be caused by a non-linearity of the dependency of the nucleophilicity on the ratio of aprotic to protic solvents, but would not be consistent with the explanation based on an equilibrium between bound methanol/methoxide as the rates should remain the same if both concentrations were increased by the same fraction.

The utilized model-based experimental analysis strategy does not allow to consider reaction steps which occur outside the catalytic cycle. Thus, the aspects and dependencies worked out in the experiments have to be incorporated directly into the catalytic cycle, see Scheme 4. It is known from DFT calculations for the Pd-TPP catalyst [32] that the addition of a strong base accelerates the rate determining step, the nucleophilic attack at complex **E**. Based on our experimental data, we conclude that the Pd-IMes catalyst requires the presence of the base to proceed the reaction. The bound methoxy is not strong enough to attack the allyl-group in an intramolecular fashion, but rather activates this part of the carbon chain for intermolecular attack by another methoxide under release of the bound methoxide. Thus, without a strong base, the reaction would stop at this point. In addition, methanol was shown to have negative influence. To account for this, we considered the nucleophilicity of the base to be represented in the adapted mechanism as a function of the protic methanol.

Scheme 4: Adapted Jolly mechanism for the IMes-modified catalyst.

With this formal modification of the Jolly mechanism, a kinetic model could be derived applying the procedure described for the TPP ligand. The resulting rate equations

$$R_1 = \frac{[Pd_{act}](K_1^{adJolly}[B]^2[KO])}{1+K_2^{adJolly}[B]^2[M][KO]+K_3^{adJolly}[B]^2[KO]+K_4^{adJolly}[B]^2[M]+K_5^{adJolly}[B]^2+K_6^{adJolly}[KO]} \quad (30)$$

for the adapted Jolly mechanism and the reduced, identifiable model

$$R_1 = [Pd_{act}]\frac{K_1^{adJolly}[B]^2[KO]}{1+K_4^{adJolly}[B]^2[M]+K_6^{adJolly}[KO]} \quad (31)$$

incorporate the dependency on the base concentration (KO). They are subsequently utilized for an additional IMI.
Table 5 shows the results of IMI for the IMes ligand with the models derived from the adapted Jolly mechanism. Based on the Akaike weights, the new derived models outperform the empirical model. This once more encourages the derivation of mechanistically motivated models for catalytic reactions. The reduced model derived from the adapted Jolly mechanism, the parameters of which are all identifiable, shows the highest Akaike weight. A graphical analysis by reaction progress analysis for this rate equation is not possible, since the reaction rates cannot be normalized to result in a function depending only on one reactant concentration. This fact underlines the advantages of the analytical approach of IMI over the graphical approach followed by reaction progress analysis. Again, a simultaneous parameter estimation with the dynamic model for the batch experiments presented above

is executed with the following rate equations for the reduced model derived from the adapted Jolly mechanism:

$$R_0 = K_0 [B]^2 \left[Pd_{pre} \right] \quad (32)$$

$$R_1 = [Pd_{act}] \frac{K_1^{adJolly} [B]^2 [KO]}{1 + K_4^{adJolly} [B]^2 [M] + K_6^{adJolly} [KO]}. \quad (33)$$

The confidence intervals of the estimated parameters shown in Table 6 together with their nominal values are less than 9 % of the nominal value, except for K_0 as expected according to the analysis above. At high to moderate butadiene concentrations, the model gives a zero-order dependency in butadiene, a first-order dependency in base and a negative influence of methanol (see Figure 9). Only at very high base concentrations, the reaction is independent of the base concentration. At the end of the reaction, when the butadiene concentration is low, the Pd-IMes catalyzed telomerization is of second-order in butadiene.

Figure 9: Results of the simultaneous parameter estimation for the IMes ligand with the reduced model for the adapted Jolly mechanism. Solid symbols and lines refer to experiments with pure 1,3-butadiene, open symbols and dashed lines to experiments with sCC_4. *Reaction conditions: 70 °C, 15 bar,* $V_{reaction}$ *= 140 ml,* $n_{butadiene}$*:*n_{Pd} *= 40000,* n_{Lig}*:*n_{Pd} *= 4,* $n_{butadiene}$*:*n_{base} *= 400,* $n_{butadiene}$*:*$n_{methanol}$ *= (black = 1:2, red = 1:3, green = 1:1, blue = 1:1.5, pink = 1:2.5).*

4 Conclusions

In the present work we have tested literature-known palladium catalysts for the telomerization of 1,3-butadiene with methanol. Two types of ligands, triphenylphosphine (TPP) and IMes were used to prepare the catalyst complex in-situ before the substrate was added. The TPP-modified complex exhibited high initial activity, but levelled off after 70 % conversion while the IMes-modified complex converted 100 % within the same period of time. Additionally, the selectivity toward the desired product 1-Mode **1** was higher when using the IMes ligand. For the first time, we compared the effect of a diluted 1,3-butadiene feed on both catalyst systems with that of pure butadiene. While the TPP-modified catalyst showed lower activity due to substrate dilution, the IMes system surprisingly showed a higher activity. This behavior could be reproduced by using inert solvents and non-reactive compounds of the sCC_4 feed. In addition, the importance of the base was shown for the Pd-IMes catalyst which does not proceed the reaction without a strong base. In addition, a strong dependence on the base concentration was found. The kinetic differences between the two ligands under investigation could be worked out by means of model-based experimental analysis. We could show that neither of them follows the dipalladium mechanism. The reaction kinetics of the Pd-TPP based catalyst were based on the Jolly mechanism showing a second-order dependency on butadiene and a first-order dependency on methanol at moderate to low butadiene concentrations and a zero-order dependency on butadiene with a first-order dependency on methanol at high butadiene concentrations. For the Pd-IMes catalyst, the reaction kinetics based on the classical Jolly mechanism did not fit the experimental data. Based on the experimental observations, the Jolly mechanism was adapted in the step where nucleophilic attack occurs in order to include the impact and necessity of the base for the IMes-based catalyst. With this formally modified mechanism, the experimental data were reproduced well, showing a zero-order dependency on butadiene at moderate to high butadiene concentrations and a first-order dependency on base while the nucleophilicity of the base is influenced by the methanol amount resulting in a negative order for methanol.

The thorough model identification procedure employed in this work also demonstrates that the derivation of mechanistically motivated models for catalytic reactions should be preferred over

blindly relying on postulated empirical models. Furthermore, this study shows that kinetic reaction progress analysis is a valuable tool, but is clearly limited in case of complex reaction mechanisms. Still, it can be a valuable tool also in these cases if it is combined with thorough model identification methodologies. In this sense, the procedures for elucidating mechanisms in complex chemical reactions and reaction kinetic modeling described in this work are of a more general nature and should be considered to better understand and optimize other catalytic reaction systems.
For the underlying study, a DFT calculation of the adapted Jolly mechanism might further support the assumed mechanism for the Pd-IMes catalyst. In addition, operando spectroscopy might help to provide additional information for a deeper, physico-chemical look inside the mechanism of possible superposition of the reaction kinetics, catalyst activation and deactivation processes.

Acknowledgements

We gratefully thank the European Community within its project SYNFLOW (FP7; grant agreement n8 NMP2-LA-2010-246461) for financial support.

References

[1] A. Behr, M. Becker, T. Beckmann, L. Johnen, J. Leschinski, S. Reyer, *Angew. Chem. Int. Ed.*, 48, (2009), 3598.
[2] S. Takahashi, T. Shibano, N. Hagihara, *Tet. Lett.*, 8, (1967), 2451.
[3] E.J. Smutny, *J. Am. Chem. Soc.*, 89, (1967), 6793.
[4] N. Yoshimura, T. Masuhiko, Process for Producing normal-Octanol, CA1174246 A1,(1984), to Kuraray Company, Ltd.
[5] R.C. Bohley, G.B. Jacobsen, H.L. Pelt, B.J. Schaart, M. Schenk, D.A. Van Oeffelen, Process for producing 1-octene, WO 1992010450 A1, (1992), to Dow Benelux N.V.
[6] P.W. Jolly, R. Mynott, B. Raspel, K.P. Schick, *Organometallics*, 5, (1986), 473.
[7] R. Jackstell, A. Frisch, M. Beller, D. Röttger, M. Malaun, B. Bildstein, *J. Mol. Catal. A: Chemical*, 185, (2002), 105..
[8] R. Jackstell, M. Gómez Andreu, A. Frisch, K. Selvakumar, A. Zapf, H. Klein, A. Spannenberg, D. Röttger, O. Briel, R. Karch, M. Beller, *Angew. Chem. Int. Ed.*, 41, (2002), 986.
[9] R. Jackstell, S. Harkal, H. Jiao, A. Spannenberg, C. Borgmann, D. Röttger, F. Nierlich, M. Elliot, S. Niven, K. Cavell, O. Navarro, M.S. Viciu, S.P. Nolan, M. Beller, *Chem. Eur. J.*, 10, (2004), 3891.
[10] F. Vollmüller, J. Krause, S. Klein, W. Mägerlein, M. Beller, *Eur. J. Inorg. Chem.*, (2000), 1825.
[11] F. Vollmüller, W. Mägerlein, S. Klein, J. Krause, M. Beller, *Adv. Synt. Catal.*, 343, (2001), 29.
[12] M.J.L. Tschan, E.J. García-Suárez, Z. Freixa, H. Launay, H. Hagen, J. Benet-Buchholz, P.W.N.M. van Leeuwen, *J. Am. Chem. Soc*., 132, (2010), 6463.
[13] M.J.L. Tschan, H. Launay, H. Hagen, J. Benet-Buchholz, P.W.N.M. van Leeuwen, *Chem. Eur. J*., 17, (2011), 8922.
[14] M.J.L. Tschan, J.-M. López-Valbuena, Z. Freixa, H. Launay, H. Hagen, J. Benet-Buchholz, P.W.N.M. van Leeuwen, *Organometallics*, 30, (2011), 792.
[15] P.W.N.M. van Leeuwen, N.D. Clément, M.J.L. Tschan, *Coord. Chem. Rev*., 255, (2011), 1499.
[16] P.W.N.M. van Leeuwen, M. Tschan, Z. Freixa, H. Hagen, Novel Phosphine-based Catalysts Suitable for Butadiene Telomerization, WO2011101504 A1, (2011), to Dow Global Technologies LLC, USA.
[17] D.G. Blackmond, *Angew. Chem. Int. Ed.*, 44, (2005), 4302.
[18] W. Marquardt, *Chem. Eng. Res. Design*, 83, (2005), 561.
[19] Y. Bard, Nonlinear parameter estimation, Academic Press, New York, 1974.

[20] A. Mhamdi, W. Marquardt, Incremental identification of distributed paramter systems, in: Advances in Chemical Engineering, Control and Optimisation of Process Systems (Volume 43), S. Pushpavanam (Ed.), Elsevier, 51-10, 2013.
[21] W. Marquardt, Identification of kinetic models by incremental refinement, in: Models, simulations, and the reduction of complexity, U. Gähde, S. Hartmann, J.H. Wolf (Eds.), Walter de Gruyter, Berlin, 2013.
[22] M. Brendel, D. Bonvin, W. Marquardt, *Chem. Eng. Sci.*, 61, (2006), 5404.
[23] A.N. Tikhonov, V.Y. Arsenin, Solutions of ill-posed problems, V. H. Winston and Sons, Washington, D.C., 1977.
[24] A. Mhamdi, W. Marquardt, An inversion approach for the estimation of reaction rates in chemical reactors, European Control Conference ECC'99, Karlsruhe, Germany, 1999.
[25] K.P. Burnham, D.R. Anderson, Model selection and multimodel inference: a practical information - theoretic approach, Springer, New York, 2002.
[26] L. Torrente-Murciano, A. Lapkin, D.J. Nielsen, I. Fallis, K.J. Cavell, *Green Chem.*, 12, (2010), 866.
[27] W. Keim, *Angew. Chem.*, 80, (1968), 968.
[28] A. Behr, G.V. Ilsemann, W. Keim, C. Krueger, Y.H. Tsay, *Organometallics*, 5, (1986), 514.
[29] J.-M. Chern, F.G. Helfferich, *AIChE J.*, 36, (1990), 1200.
[30] K.A.P. McLean, K.B. McAuley, Canad. J. Chem. Eng.,, 90, (2012), 351.
[31] T. Quaiser, M. Mönnigmann, *BMC Systems Biology*, 3, (2009), 50.
[32] A. Jabri, P.H.M. Budzelaar, *Organometallics*, 30, (2011), 1374.

Table 1: Telomerization results obtained for two feeds and two different palladium catalysts after 6 h reaction time.

Feed	Ligand	X / %	Y_1 / %	Y_2 / %	Y_3 / %	S_1 / %	S_{1+2} / %	*n*:*iso*	TON
1,3-butadiene	TPP	95.7	83.2	8.2	3.9	87	95.5	10.2	38311
sCC_4	TPP	76.2	64.4	6.5	4.9	84.5	93.1	9.9	30562
1,3-butadiene	IMes	99.1	96.7	1.7	0.4	97.6	99.4	55.5	39676
sCC_4	IMes	99.9	97.3	1.6	0.4	97.5	99.1	59.7	39925

Definition of abbreviations: X = conversion, Y = Yield, S = selectivity, TON = turnover number.

Table 2: Results of incremental model identification for the TPP ligand.

	rate equations	Akaike weights
Jolly mechanism	$R_1 = [Pd_{act}] \frac{K_1^{Jolly}[B]^2[M]}{1 + K_2^{Jolly}[B]^2 + K_3^{Jolly}[B]^4}$	
	$R_2 = [Pd_{act}] \frac{K_4^{Jolly}[M][B]^2(1 + K_5^{Jolly}[B]^2)}{1 + K_6^{Jolly}[B]^2 + K_7^{Jolly}[B]^4}$	0.015
reduced Jolly mechanism	$R_1 = [Pd_{act}] \frac{K_1^{Jolly}[B]^2[M]}{1 + K_2^{Jolly}[B]^2}$	
	$R_2 = [Pd_{act}] K_4^{Jolly}[M][B]^2$	0.814

dipalladium mechanism $R_1 = [Pd_{act}] \frac{K_1^{Dipa}[M][B]^2}{1 + K_2^{Dipa}[M]}$

$$R_2 = [Pd_{act}] \frac{K_3^{Dipa}[B]^2}{1 + K_4^{Dipa}[M]}$$

0.02

reduced dipalladium mechanism $R_1 = [Pd_{act}] K_1^{Dipa}[M][B]^2$

$$R_2 = [Pd_{act}] K_3^{Dipa}[B]^2$$

0.15

empirical $R_1 = K_1^{Emp}[B]^{K_2^{Emp}}[M]^{K_3^{Emp}}[Pd_{act}]^{K_4^{Emp}}$

$$R_2 = K_1^{Emp}[B]^{K_6^{Emp}}[M]^{K_7^{Emp}}[Pd_{act}]^{K_8^{Emp}}$$

0.001

Table 3: Parameter values and confidence intervals for TPP ligand after simultaneous correction step.

parameter	estimated value	95% confidence interval
K_0	0.75	0.23
K_1^{Jolly}	66.1	1.6
K_2^{Jolly}	0.03	0.002
K_4^{Jolly}	3.19	0.3

Table 4: Results of incremental model identification for the IMes ligand.

rate equations	Akaike weights
Jolly mechanism $R_1 = [Pd_{act}] \frac{K_1^{Jolly}[B]^2[M]}{1 + K_2^{Jolly}[B]^2 + K_3^{Jolly}[B]^4}$	0.019
reduced Jolly mechanism $R_1 = [Pd_{act}] \frac{K_1^{Jolly}[B]^2[M]}{1 + K_2^{Jolly}[B]^2}$	0.054
dipalladium mechanism $R_1 = [Pd_{act}] \frac{K_1^{Dipa}[M][B]^2}{1 + K_2^{Dipa}[M]}$	<0.001
reduced dipalladium mechanism $R_1 = [Pd_{act}] K_1^{Dipa}[M][B]^2$	<0.001
empirical $R_1 = K_1^{Emp}[B]^{K_2^{Emp}}[M]^{K_3^{Emp}}[Pd_{act}]^{K_4^{Emp}}$	0.926

Table 5: Results of incremental model identification for IMes ligand with models derived from the adapted mechanism.

rate equations	Akaike weights
Jolly mechanism $R_1 = [Pd_{act}] \frac{K_1^{Jolly}[B]^2[M]}{1 + K_2^{Jolly}[B]^2 + K_3^{Jolly}[B]^4}$	<0.001

reduced Jolly mechanism $R_1 = [Pd_{act}] \frac{K_1^{Jolly} [B]^2 [M]}{1 + K_2^{Jolly} [B]^2}$

<0.001

dipalladium mechanism $R_1 = [Pd_{act}] \frac{K_1^{Dipa} [M][B]^2}{1 + K_2^{Dipa} [M]}$

<0.001

reduced dipalladium mechanism $R_1 = [Pd_{act}] K_1^{Dipa} [M][B]^2$

<0.001

empirical $R_1 = K_1^{Emp} [B]^{K_2^{Emp}} [M]^{K_3^{Emp}} [Pd_{act}]^{K_4^{Emp}}$

0.001

adapted Jolly mechanism

$R_1 = [Pd_{act}] \frac{K_1^{adJolly} [B]^2 [KO]}{1 + K_2^{adJolly} [B]^2 [M][KO] + \ldots}$ 0.048

reduced adapted Jolly mechanism $R_1 = [Pd_{act}] \frac{K_1^{adJolly} [B]^2 [KO]}{1 + K_4^{adJolly} [B]^2 [M] + K_6^{adJolly} [KO]}$

0.951

Table 6: Parameter values and confidence intervals for the IMes ligand after simultaneous correction step.

parameter	estimated value	95% confidence interval
K_0	620	>1000
$K_1^{adJolly}$	50.3e6	41e4
$K_4^{adJolly}$	19.3	1.6
$K_6^{adJolly}$	3417	292